RADIOWAVE SCATTERING FROM SURFACE ROCKS: APPLICATION TO MARS VIKING AND PATHFINDER LANDING SITES. J. E. Baron, *johnb@nova.stanford.edu*, R. A. Simpson, G. L. Tyler, *Center for Radar Astronomy, Stanford University, Stanford CA 94305-9515, USA.*

While interpretive models for radiowave scattering from gently undulating regions of planetary surfaces have been available for some time [1], the effects of discrete, wavelength-scale surface structure (*e.g.*, rocks) are difficult to incorporate into a theoretical framework. Analytic solutions for scattering from canonical objects, such as spheres, resting on or buried a dielectric half-space (a planetary regolith) are available only in limiting cases for which (i) the objects are small compared to the wavelength of the incident radiation; (ii) the objects are large compared to the wavelength; or (iii) the dielectric contrast between the object and the surface vanishes. Since radar waves interact most strongly with objects on the order of a wavelength in size, these solutions are of limited utility for interpretation of remote surface sensing data. Another approach is to model rocks as spheres in an infinite background medium and use standard Mie theory, in conjunction with appropriate Fresnel transmission and penetration depth factors, to estimate cross sections [2]. However, even if all rocks were spherical in shape, the validity of this approximation is difficult to determine. Our approach is to use computer models to study scattering for these geometries.

Over the past few years we have been developing a numerical model, based on finite-difference time-domain (FD-TD) techniques, for studying scattering from objects of arbitrary shape and composition in the presence of a dielectric half-space. Details of the implementation are described elsewhere [3]; two-dimensional (2-D) simulations of scattering from cylinders show the marked effect of the regolith relative to free space solutions [4]. We used results from our 2-D calculations to estimate cross sections for the Viking Lander sites [5]; while 2-D solutions computationally are inexpensive to obtain, they require the introduction of several scaling factors to account for polarization effects and conversion from two to three dimensions. With the maturation of our three-dimensional (3-D) code, we are in a position now to join the discussion with more substantive results.

The primary advantages of the 3-D code are that polarization effects can be examined in detail and that realistic rock shapes can be modeled. We present a few examples here. Figure 1 depicts the geometry for our scattering calculations; for our material and geometrical parameters, we let $\epsilon_d = 4$, $\epsilon_1 = 2.56$, and $\theta_i = \theta_s = 45^\circ$ (*i.e.*, backscatter). Figure 2 shows the backscatter cross section of a sphere of radius a for three distinct depths over a range of sizes, which are centered around a diameter $2a = \lambda$. Also shown are Mie solutions for the same sphere in free space and in an infinite background medium with permittivity ϵ_1. Note the two- to three-order magnitude difference in scattered power between

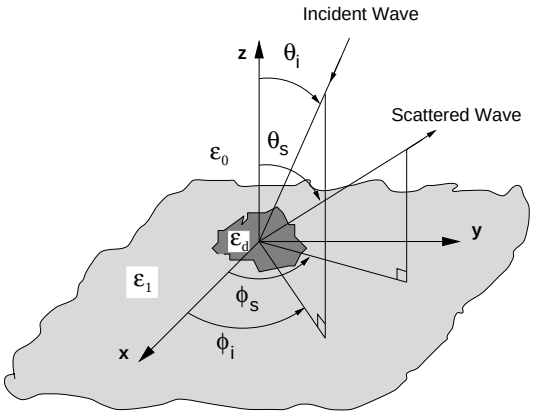

Figure 1: Geometry for 3-D Scattering Calculations. The incident wave arrives from a direction with polar coordinates (θ_i, ϕ_i); the scattered wave is calculated at (θ_s, ϕ_s). The dielectric constant of the surface is ϵ_1, while that of the scattering object is ϵ_d. The scattering object may rest on the surface, or be partially or fully buried.

the surface sphere and the buried sphere; also note that the thick dashed line is nearly the same as the result for the buried sphere, offset by about 7 dB. Buried spheres can be modeled reasonably well using Mie theory and simple scale factors. Similar results were obtained with the 2-D code.

The results in Fig. 2 correspond to a horizontally polarized incident wave. By performing a similar calculation for a vertically polarized incident wave, we can synthesize arbitrary transmitter/receiver polarization configurations, such as right and left circular polarization. In Fig. 3 we calculate the circular polarization ratio, $\mu_c = \sigma_{sc}/\sigma_{oc}$, for the sphere at various depths; μ_c is the cross section ratio of the same ("unexpected") sense of circular polarization to the opposite ("expected") sense and is considered a measure of small-scale roughness. The cross sections were averaged over $ka = \pm\pi/8$ before taking the ratio in order to smooth the results. For these parameters the polarization ratio is significantly higher for surface and partially buried spheres than for buried spheres, although the ratio never exceeds 0.3.

Since it is rare to find rocks of spherical shape in practice, we are also examining more realistic models. Based on rock population data from the Viking Lander sites [6], we have calculated that typical axial ratios for Martian rocks at these sites are 1 (length) : 0.7 (width) : 0.5 (height). Using a 3-D laser scanner available at the

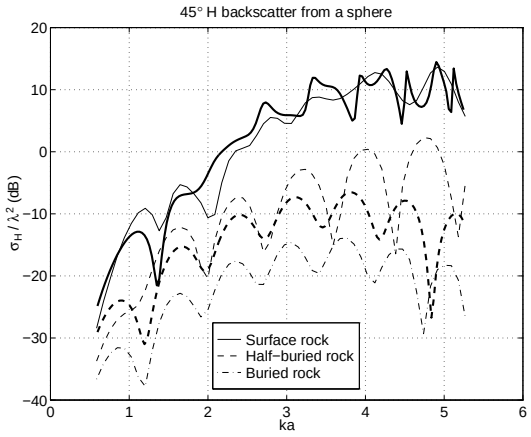

Figure 2: Backscatter RCS from a Sphere vs. Radius. The backscatter cross section of a sphere over a range of sizes $ka = 2\pi a/\lambda$, where a is the sphere radius, is shown for three different depths: resting on the surface, half-buried, and tangentially buried beneath the surface. The incident wave is horizontally polarized. The thick solid line is the Mie solution in free space; the thick dashed line is the Mie solution for the same object immersed in an infinite background medium of permittivity 2.56.

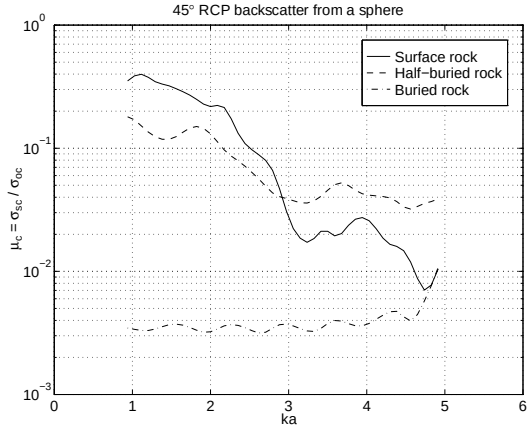

Figure 3: Circular Polarization Ratio for a Sphere vs. Radius. Results are shown for three burial depths. Note that the cross sections have been filtered before calculating μ_c.

Stanford Computer Graphics Laboratory, we have made accurate digital models of several terrestrial rocks, some of which have the axial ratios indicated above. Figure 4 shows the calculated circular polarization ratio versus size and depth for one such rock, where the volume of the rock is equivalent to that of the sphere considered in Figs. 2–3. In this case, instead of averaging over size, we have averaged over azimuthal angle ϕ_i ($= \phi_s$) since each azimuthal angle is essentially a different "look." Again, the surface object depolarizes the incident radiation more strongly than the buried object does.

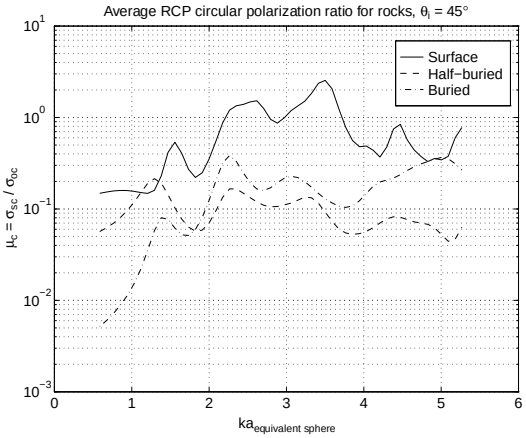

Figure 4: Circular Polarization Ratio for a Rock vs. Size. Results are given for three burial depths. Rather than averaging over size, cross sections have been averaged over azimuthal orientation before the μ_c calculation.

These types of 3-D results should provide a more fundamental basis for calculating cross sections both at Mars landing sites and elsewhere on planetary surfaces where rock populations are significant.

References

[1] Beckmann P. and Spizzichino A. (1963) *The Scattering of Electromagnetic Waves from Rough Surfaces*, Pergamon Press.

[2] Harmon J.K. and Ostro S.J. (1985) Icarus 62, 110.

[3] Wong P.B. *et al.* (1996) IEEE Trans. Ant. and Prop., 44, 504.

[4] Baron J.E. *et al.* (1996) Icarus, 122, 383.

[5] Simpson R.A. *et al.* (1996) *LPSC XXVII*, 1205.

[6] Moore H.J. and Keller J.M. (1991) Reports of the PGGP, NASA TM-4300, 160.